Journal of King Saud University – Science 34 (2022) 101831

Contents lists available at ScienceDirect

Journal of King Saud University – Science

journal homepage: www.sciencedirect.com

Original article

Synthesis and characterization studies of pure and Ni doped CuO nanoparticles by hydrothermal method

M. Chandrasekar [a], M. Subash [b], S. Logambal [b], G. Udhayakumar [c], R. Uthrakumar [b], C. Inmozhi [d,*], Wedad A. Al-Onazi [e], Amal M. Al-Mohaimeed [e], Tse-Wei Chen [f], K. Kanimozhi [g]

[a] Department of Physics, Periyar University, Salem - 636011, Tamil Nadu, India
[b] Department of Physics, Govt. Arts College (Autonomous), Salem - 636007, Tamil Nadu, India
[c] Department of Physics, Arignar Anna Govt. Arts College, Villupuram - 605602, Tamil Nadu, India
[d] Department of Physics, Govt. Arts College for Women, Salem - 636008, Tamil Nadu, India
[e] Department of Chemistry, College of Science, King Saud University, P.O. Box 22452, Riyadh 11495, Saudi Arabia
[f] Department of Materials, Imperial College London, London SW7 2AZ, United Kingdom
[g] Department of Chemistry, Global Institute of Engineering and Technology, Melvisharam - 632509, Tamil Nadu, India

ARTICLE INFO

Article history:
Received 18 November 2021
Revised 3 January 2022
Accepted 9 January 2022
Available online 15 January 2022

Keywords:
Copper oxide
Nanoparticles
Hydrothermal
X-ray diffraction
Magnetic properties
Dielectric and PL studies

ABSTRACT

An efficient synthesis of Ni doped CuO nanoparticles were carried out by hydrothermal method. The prepared material was subjected to X-ray diffraction (XRD), the morphological characteristics of the prepared material system were studied by scanning electron microscope (SEM) technique. FTIR spectra have confirmed the establishment of CuO nanoparticles. Optical absorption spectra of prepared nanoparticles were measured using UV–vis spectroscopy and photoluminescence (PL) studies. A thorough examination of the frequency dependent dielectric constant reveals the unique impact of various polarizations. According to the magnetic experiments, the produced nanoparticles had a maximal magnetic moment value of 5.0 wt% for Ni doped CuO Nps. All the above analysis were studied the grain size were found and calculated for pure CuO, Ni incorporated CuO respectively.

1. Introduction

The research of nanostructures can deliver extraordinary understanding of materials and devices, nanostructures reveal novel and significantly improved physicochemical properties, and processes compared to their majority counterparts (Khan et al., 2013; Kaviyarasu et al., 2012; Ahamed et al., 2014; Ghulam et al., 2013; Kida et al., 2007). Nanoparticles seem to become increasingly significant as they benefit an extensive choice of scientific disciplines due to its light weight in nanometres (Kim et al., 2008; Anandan and Yang, 2007; Zhang et al., 2014; Kaviyarasu et al., 2013). The development, construction, and use of multiple functions having at least one distinctive nanometer scale is referred to as nanotechnology (Suleiman et al., 2013; Kaviyarasu et al., 2016). The copper oxide (CuO-NPs) nanoparticle is a useful metal oxide with several uses in domains including such nanofluids, heat transmission, and associated devices (Angel Ezhilarasi et al., 2018; Ramesh et al., 2021; Manimaran et al., 2014). Nanomaterials have widely differing qualities beyond what they exhibit at the macro or micro sizes due to its unique features, and they will be widely employed in several applications (Albadi et al., 2013; George et al., 2020). CuO has the rare feature of acting as a semiconductor, semiconductor materials particularly attracted the attentions of researchers due to its significant utility in electrical and optoelectronic procedures such as electrochemical cells, gas sensors, magnetic storage devices, and catalysts (Anand et al., 2021; George et al., 2022; Nithiyavathi et al., 2021; Zhou et al., 2013; Joshua et al., 2014; Panimalar et al., 2022; Darezereshki and Bakhtiari, 2011). The CuO-NPs have been used in dye removal, nanoparticulate film production, gas sensors, semiconductors, organic catalysis, solar energy transformation, and several other applications (Yuan et al., 2007; Saravanakkumar et al., 2019; Rathnakumar et al., 2019; Kana et al., 2019). The CuO-NPs can also be used in heat

* Corresponding author.
E-mail addresses: cinmozhi@gmail.com, cvesta19@yahoo.com (C. Inmozhi).
Peer review under responsibility of King Saud University.

Production and hosting by Elsevier

https://doi.org/10.1016/j.jksus.2022.101831
1018-3647/

exchange, the heat transfer of CuO-based nanofluid is 12.4 percent greater than that of deionized water (Lim et al., 2012; Wang et al., 2002; Poizot et al., 2000). The focus of the study was to synthesise nanosized pure copper oxide and Ni doped CuO powder in a simple and efficient manner, and to probe crystallite size, crystallinity, shape, microstructure, morphology, and interactions seen among lifeforms of CuO-NPs, the existence of metal dopants, and the resemblance of pure and doped CuO NPs (Katti et al., 2003; Panimalar et al., 2020; Carnes and Klabunde, 2003). CuO and metal-incorporated CuO-NPs were produced in this work using a hydrothermal technique, temperatures below the melting point at temperatures of 600 °C (Volanti et al., 2008; Fan et al., 2004; Yang et al., 2003). These have been observed that adding 4% CuO to water enhances its thermal conductivity by 20%. CuO is a semiconductor with a small bandgap that is utilised in photoconductive and photodynamic applications (Lee et al., 1999; Borgohain et al., 2014; Rahmana et al., 2011; Liu et al., 2006). The Ni metal ion incorporated CuO's favourable bandgap (1.0 eV to 2.08 eV) renders it helpful for photovoltaic devices and may be utilised to create solar panel windows. In this paper, we used the efficient hydrothermal procedure to make CuO nanoparticles. Powder XRD, SEM with EDAX, FTIR, UV–vis, PL, Dielectrics, and VSM investigations have been carried out to characterise the produced nanoparticles extensively.

2. Experimental procedure

2.1. Synthesis of pure and doped CuO nanoparticle

The pure and metal doped CuO nanoparticles were prepared by a low temperature hydrothermal route. To prepare CuO, 0.5 M of copper sulphate was dissolved in 50 ml doubly de-ionized water and kept in vigorous mixing for 30 min. An appropriate amount of sodium hydroxide solution (NaoH) was added drop by drop to the prepared mixture to attain the 8.5 pH value of the mixture solution and again stirred for 3 h to form homogeneous solution. The prepared solution was transformed in Teflon lined stainless steel autoclave and kept in heating furnace which is upheld at 180 °C for 12 h, then the mixer was allowed to cool, the dark brown precipitate was extracted. The harvested precipitate was splashed multiple times with distilled water and ethanol to remove contaminants and finally dried in hot air oven at 80 °C for 12 h to gain CuO nanoparticles. For metal doped CuO, 5 wt% of Nickel sulphate was added by impregeration method by using the above procedure for Ni metal doped CuO nanoparticle.

2.2. Characterisations studies

Using an X-ray spectra were recorded, X-ray diffraction (XRD) has been used to examine the phases to determine the crystalline part of the materials. (XRD, Bruker D8 Advance, Germany) by a Cu-K_α radioactive source of 0.15405 nm in the 2 range of 20° to 80°. The XRD results were obtained with diffraction intensity versus 2 theta. Scanning electron microscopy was employed to determine the surface topography of the samples (JEOL, JSM-7600F, Japan). For elemental analysis, an energy dispersive X-ray (EDAX) study was conducted using a JEOL JSM-7600F. The material was FTIR spectroscopically examined in the 400–4000 cm^{-1} range (with Perkin Elmer 1650, USA) using a Thermo-Nicolet Avatar 370 model FTIR to better comprehend the structural and chemical characteristics of pure CuO and Ni doped CuO nanoparticles. The bandgap was calculated after recording energy dispersive spectra using a UV–visible spectrophotometer. Photoluminescence (PL) spectra were obtained in the 400–800 nm region. As we added metal oxide nanoparticles, we saw substantial improvements in the Hall Effect and vibrating sample magnetometer (VSM), as well as a considerable improvement in dielectric characteristics.

3. Results and discussion

3.1. Powder X-ray analysis

Fig. 1 depicts the characterisation of X-ray diffraction peaks of pure and doped materials of CuO nanoparticles with changing concentration of Ni doped CuO nanoparticles observed in the range of 2 between 20° and 80°. The powder XRD pattern was used to describe the acquired materials, which were acquired using a Schimadzu model XRD 6000 with CuK_α radiation (λ = 1.5417 Å). The crystallographic planes validated the material's crystalline phase and are very well aligned to specifications (JCPDS – card # 05 – 0661). The result shows the characteristics diffraction peaks located at 2θ = 22.75°, 28.31°, 35.65°, 38.59°, 41.14°, 46.32°, 52.55°, 61.49°, 66.37°, and 72.17°. There really is no discernible shift in peak location, and the spikes are observed to be extremely acute and powerful. The Debye Scherrer equation was used to compute the regular crystalline sizes of pure CuO and Ni doped CuO. The usual crystallite size rises somewhat as the quantity of doped Ni concentration increase, ranged from 18 to 28 nm respectively.

3.2. Scanning electron microscopic (SEM) studies

The morphology of pure CuO nanoparticles and Ni doped CuO nanoparticles was studied using scanning electron microscopy. The nanoflower-like shape used in this study enables for more results from a combination of reactant molecules to much more active areas, improve the effectiveness of photocatalysis. As shown in Fig. 2 pure CuO looks flower – like morphology nanostructure. From Fig. 3 Ni doped CuO reveal the formation of nanoparticle with size ranging from 19 to 28 nm. It is critical to notice that by changing the proportion of Ni iron inside the parental CuO, the morphology shifts from nanoflowers to nanoplates and finally to nanoparticles.

3.3. Energy dispersive X-ray (EDX) analysis

The resultant solution for pure CuO and Ni doped CuO samples was examined utilizing energy dispersive X-ray analysis, as seen in Fig. 3a and b. CuO nanoparticles were analysed by EDX at 10 keV. The existence of copper (Cu) and oxygen (O) elements was discovered in CuO NPs, with results suggested that the nanoparticles

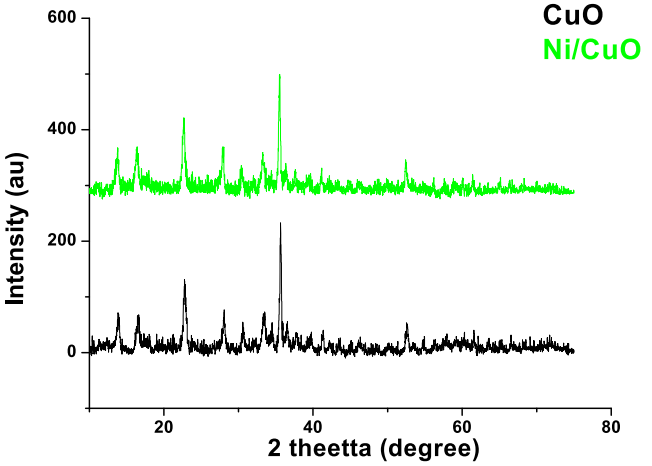

Fig. 1. X-ray diffraction pattern of pure and Ni doped CuO nanoparticles.

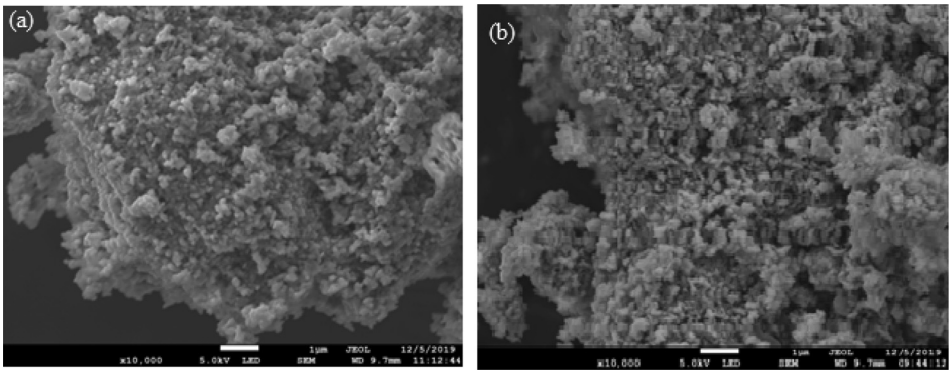

Fig. 2. (a) SEM image pure CuO nanoparticle; (b) SEM image of Ni doped CuO nanoparticles.

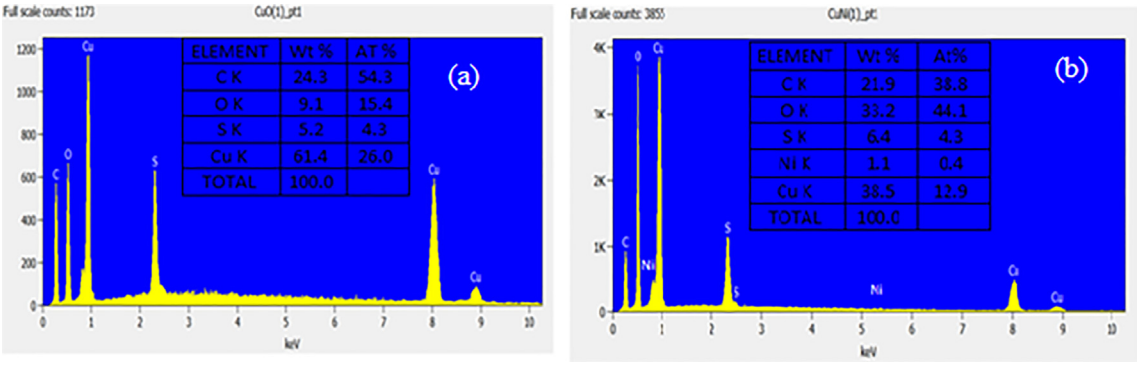

Fig. 3. (a) EDX spectrum of pure CuO; (b) EDX spectrum of Ni doped CuO nanoparticles.

remained almost stoichiometric. The mass percentage of copper and oxide determined from EDX examination were Cu 61.4 wt% percent (0.804 keV) and Cu 61.4 wt% percent (0.804 keV), correspondingly, and no additional elemental impurities were found as pure EDX spectrum. From Fig. 3b Ni-doped CuO NPs occurrence of copper (cu), oxygen (O) and nickel sulphate (Ni) elements in CuO NPs. The Ni doped CuO indicates the weight % are calculated from EDX analysis were (nickel sulphate) Ni 1.1 wt% (0.4 keV) the values are tabulated respectively. This finding validated the synthesis of pure CuO nanoparticles.

3.4. Fourier Transformation Infra-Red (FTIR) analysis

The Fig. 4 shows the FTIR spectra of pure and Ni doped CuO nanoparticles. From the spectrum the peaks 3000 cm^{-1} to 3500 cm^{-1} are due to bending oscillations of OH groups which generally semi conducted nanostructure material absorbed in the surface owing to its mesoporous arrangement (Kana et al., 2019; Zheng and Liu, 2007). In the spectrum of CuO dual frequency crests at 596 and 521 cm^{-1} relates to M–O band vibration frequency supports that the presence of monoclinic phases (Lim et al., 2012; Mehedi Hassan et al., 2015). The vibrational characteristics of CuO nanostructures were allocated to the low frequency range 400–700 cm^{-1} in the current study. Due to the sheer oxygen stretching vibration frequencies, there really is no peaks between 1500 and 3300 cm^{-1}. Peaks at 525 and 580 cm^{-1} in the FTIR spectra of CuO-NPs have been observed and are very well aligned with findings (Rathnakumar et al., 2019; Chandrasekar et al., 2021). As a result, the metal–oxygen occurrences measured for pure and doped CuO-NPs are quite identical to those described in the literature (Rehman et al., 2011; Poovendran et al., 2020; Jeyaram et al., 2020; Senthil et al., 2020).

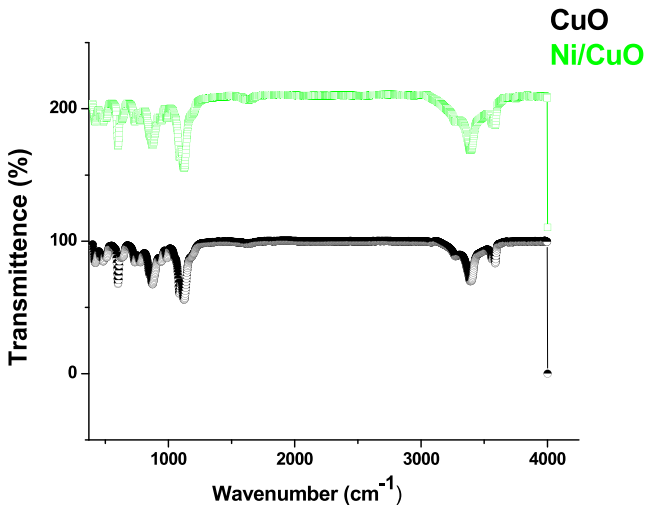

Fig. 4. FTIR spectrum of pure and Ni doped CuO nanoparticles.

3.5. Photoluminescence studies

The morphological attributes of a materials may be easily spotted by optical research, in which the prevalence of imperfections and surface states vary based on the synthesizing circumstances, types of dopant and concentrations, particle size and shape, and so on (Jing et al., 2012). The apparent emissions of pure and Ni doped CuO nanoparticles in the range 300–550 nm is referred to the electron transfer driven by structural defects in the bandgap, including oxygen - containing functional groups, based on the spectrum (Fig. 5). Optoelectronic systems could benefit from

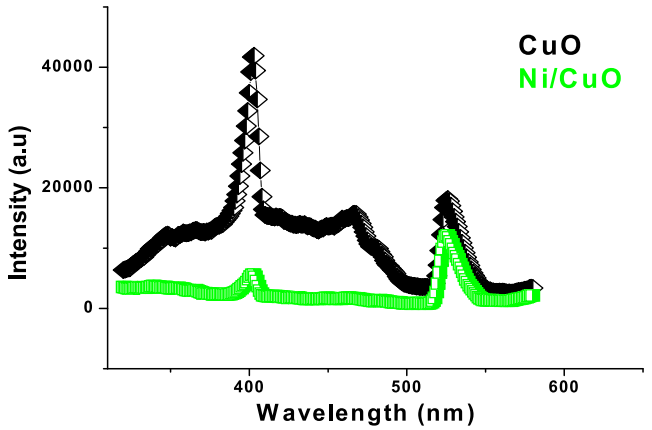

Fig. 5. Photoluminescence spectrum of pure and Ni doped CuO nanoparticles.

visible emission. Particularly, profound donors in semiconductor oxide cause the development of new energy state in the bandgap found in produced pure and doped CuO nanostructures (Wang et al., 2002). These bands at 410 and 630 nm fit correctly to the previously defined emission bands of CuO NPs due to electron interaction with holes contained in singularly ionised oxygen – containing functional groups of Ni doped CuO.

3.6. UV–vis studies

The UV–vis spectroscopy is an essential quasi approach for determining the energy deficit of semiconducting nanostructures, and it was used to investigate the optical characteristics of pure and Ni doped CuO NPs. Fig. 6 depicts the UV–visible spectrum of produced pure and Ni doped CuO nanoparticles, as well as the absorption of all samples in the frequency range of 200–800 nm. The absorption spectrum edges have moved slightly towards longer wavelength (1.45–1.20 eV) after doping Ni with CuO up to 5% wt mol. This assignment of absorbance is primarily determined by factors such as particle diameter, oxygen deficit, lattice parameters and depth, and so on (Poizot et al., 2000; Katti et al., 2003; Panimalar et al., 2020). As a result, the energy variance between both the value band and the conduction band widens as concentration decreases. The pure CuO and Ni doped CuO NPs had wide absorption peaks at 240 and 245 nm, as seen in the figure. Therefore, we determined that proportion of Ni doped CuO NPs has superior optical properties when compared to pure CuO NPs (see Fig. 7).

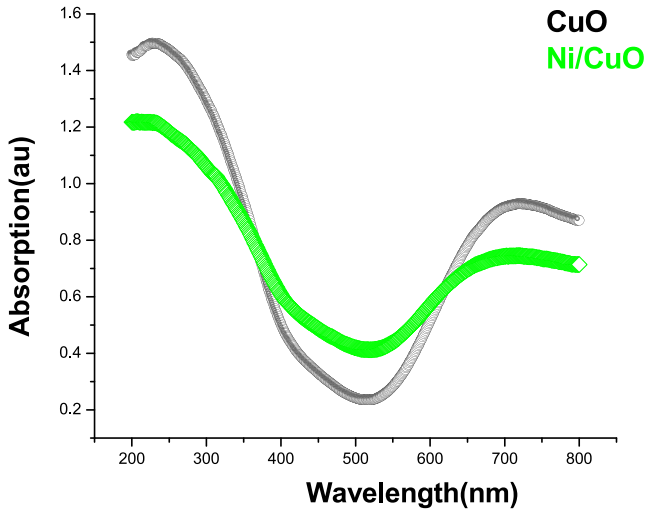

Fig. 6. UV–vis spectrum of pure and doped CuO nanoparticles.

3.7. Dielectric studies

The dielectric properties of these materials are critical for studying the crystalline movements of the material. Therefore HIOKI 3532–50 LCR HITESTER was used to evaluate the dielectric properties of pure CuO and doped Ni/CuO nanomaterials. To achieve a satisfactory surface polish, the selected samples were treated with fine-grade alumina powder. This formula is used to determine the dielectric properties (see Fig. 8).

$$\varepsilon = \frac{cd}{A\varepsilon_0} \tag{1}$$

where C denotes capacitance, d denotes thickness, A is area, and 0 is the pure permeability of empty space, which is 8.854×10^{-12} F/m. To use the relationship, the imaginary dielectric constant1 was determined.

$$\varepsilon = \varepsilon \tan\delta \tag{2}$$

Dielectric investigations give information on the dielectric constant that results from the involvement of different polarizations, such as electronic, ionic, atomic, space charge, and so on, that emerge in a material when subjected to electric field changes. The existence of charge density polarisation accounts for the high dielectric constant at low frequencies. An examination of the wavelength dependant dielectric constant reveals the unique impact of various polarizations. The minimum level of electrical resistivity at higher frequency indicates that the materials have good magnetic properties with fewer defects, and this characteristic is critical for magnetic applications of pure and Ni metal ions doped CuO (Rao et al., 2007; Saravanakkumar et al., 2018; Kaviyarasu et al., 2015).

3.8. VSM (Vibrational Sample Magnetometry)

Vibrating Sample Magnetometry was used to evaluate the magnetic characteristics of CuO and doped Ni/CuO at room temperature (VSM). At ambient temperature, the material exhibits good nonlinear characteristics and a distinct ferromagnetic behaviour with ferromagnetic order, as seen in the Fig. 9. It was discovered in nanoparticles of copper oxide and nickel doped copper oxide.

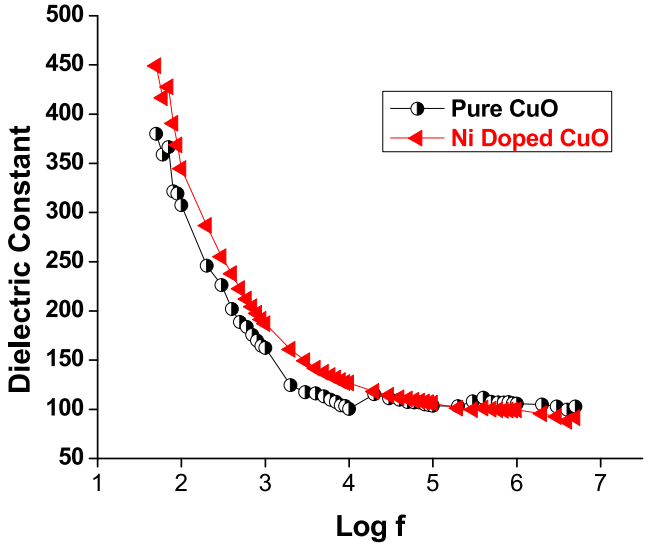

Fig. 7. Dielectric constant *vs* log f of CuO nanoparticles.

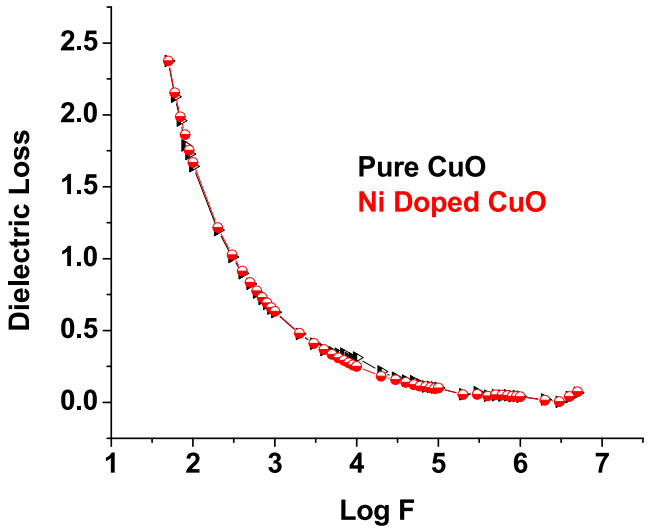

Fig. 8. Dielectric Loss *vs* log f of CuO nanoparticles.

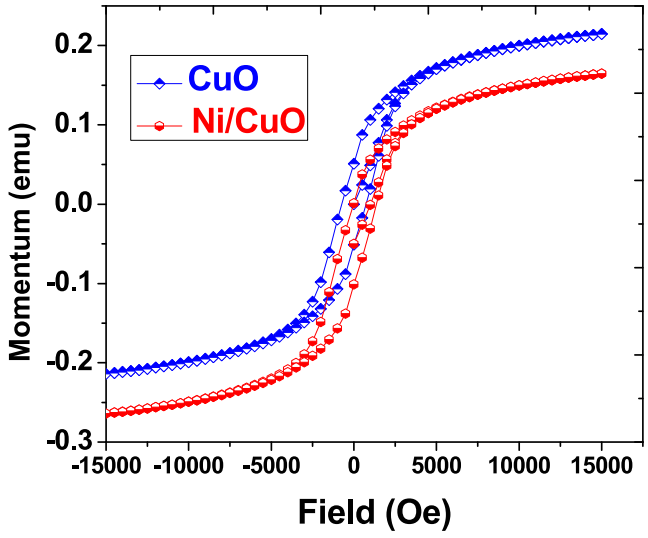

Fig. 9. M-H loops of pure and Ni doped CuO nanoparticles at room temperature.

We understand that the magnetic characteristics of pure CuO are governed by their dimension (Panimalar et al., 2020), and that it performs like ferromagnetic materials (Carnes and Klabunde, 2003). The m(H) curves of pure CuO nanoparticles show the prevalence of ferromagnetic structure, with a instant intensity of 0.047 emu/g, which really is consistent with earlier studies. Furthermore, as seen in the figure, that magnetic moment of the produced models surges with doped Ni. Because of the increased super interchange relations of Ni-O-Cu couplings, the hysteresis behaviour of Ni doped samples is significantly improved. Nevertheless, due to the nanoparticles Ni doped CuO, doping of Ni ions occurs, resulting in a massive magnetic moment and ferromagnetism (Kaviyarasu et al., 2015; Theophil Anand et al., 2019; Jayakumar et al., 2022; Kayalvizhi et al., 2022). As a result, we may infer that this structure permits ambient temperature ferromagnetism, which could be explored for spin-based purposes.

4. Conclusions

The current experiment shows the effective production of pure CuO and Ni doped CuO NPs using a hydrothermal technique that uses less expensive materials and ease of operation. The refining of X-ray diffraction patterns indicated the development of pure CuO monoclinic phase in the occurrence of Ni doped content up to 5.0 wt% percent replace ions. The crystalline size ranges from 19 to 28 nm. On pure and Ni doped CuO content, SEM examination revealed the development of clear spherical-like flowers fashioned with nanoparticles. EDX analysis verified the essential quantity and stoichiometry ratio of CuO NPs. The existence of organic compounds such as metal oxygen bonds was confirmed by the FTIR spectra. The photoluminescence spectrum used to characterize the samples show a characteristic peak at 450 nm, which would be ascribed to the existence of charge transfer emission peaks in several optical examinations. The conduction and concentration of pure and metal ion inserted CuO are determined by the UV–visible spectral light. According to magnetic studies, the inclusion of Ni ions increases the magnetic properties of the sample. The minimal concentration of dielectric loss at high frequencies indicates the material's good magnetic properties. The typical investigations show that the produced candidate is a difficult one that is highly appropriate for situations in opto-electric, sensor gas, optical, LED, solar cells, and magnetic associated devices.

CRediT authorship contribution statement

M. Chandrasekar: Investigation, Methodology, Project administration. **M. Subash:** Writing – original draft, Writing – review & editing. **S. Logambal:** Writing – original draft, Writing – review & editing. **G. Udhayakumar:** Data curation, Writing – review & editing. **R. Uthrakumar:** Supervision, Validation. **C. Inmozhi:** Investigation, Methodology, Supervision, Data curation, Writing – review & editing. **Wedad A. Al-Onazi:** Visualization, Funding acquisition. **Amal M. Al-Mohaimeed:** Visualization. **Tse-Wei Chen:** Visualization. **K. Kanimozhi:** Visualization.

Declaration of Competing Interest

The authors declare that they have no known competing financial interests or personal relationships that could have appeared to influence the work reported in this paper.

Acknowledgement

The authors extend their appreciation to the Researchers Supporting Project Number (RSP2022R469), King Saud University, Riyadh, Saudi Arabia.

References

Ahamed, M., Alhadlaq, H.A., Khan, M.A.M., Karuppiah, P., Al-Dhabi, N.A., 2014. Synthesis, characterization and antimicrobial activity of copper oxide nanoparticles. J. Nanomater. 2014, 1–4.
Albadi, J., Mansournezhad, A., Abbaszadeh, H., 2013. CuO-CeO2 nano composite: a highly efficient recyclable catalyst for the green synthesis of 1, 8dioxooctahydroxanthenes in water. J. Chin. Chem. Soc. 60, 1193–1206.
Anand, G.T., Sundaram, S.J., Kanimozhi, K., Nithiyavathi, R., Kaviyarasu, K., 2021. Microwave assisted green synthesis of CuO nanoparticles for environmental applications. Mater. Today:. Proc. 36, 427–434.
Anandan, S., Yang, S., 2007. Emergent methods to synthesize and characterize semiconductor CuO nanoparticles with various morphologies-an overview. J. Exp. Nanosci. 2, 23–56.
Angel Ezhilarasi, A., Judith Vijaya, J., Kaviyarasu, K., John Kennedy, L., Ramalingam, R.J., Al-Lohedan, H.A., 2018. Green synthesis of NiO nanoparticles using Aegle marmelos leaf extract for the evaluation of in-vitro cytotoxicity, antibacterial and photocatalytic properties. J. Photochem. Photobiol., B 180, 39–50.
Borgohain, K., Singh, J.B., Rama Rao, M.V., Shripathi, T., Mahamuni, S., 2014. Quantum Size Effects in CuO Nanoparticles. Phys. Int. J. Sci. Eng. Res. 5, 2229–2239.
Carnes, C.L., Klabunde, K.J., 2003. The catalytic methanol synthesis over nanoparticle metal oxide catalysts. J. Mol. Catal. A Chem 194 (1-2), 227–236.

Chandrasekar, M., Panimalar, S., Uthrakumar, R., Kumar, M., Raja Saravanan, M.E., Gobi, G., Matheswaran, P., Inmozhi, C., Kaviyarasu, K., 2021. Preparation and characterization studies of pure and Li+ doped ZnO nanoparticles for optoelectronic applications. Mater. Today Proceed. 36, 228–231.

Darezereshki, E., Bakhtiari, F., 2011. A novel technique to synthesis of tenorite (CuO) nanoparticles from low concentration CuS_O4 solution. J. Min. Metal., Sect. B. 47, 73–79.

Fan, H., Yang, L., Hua, W., Wu, X., Wu, Z., Xie, S., Zou, B., 2004. Controlled synthesis of mono dispersed CuO nanocrystals. Nanotechnology 15 (1), 37–42.

George, A., Raj, D.M.A., Raj, A.D., Irudayaraj, A.A., Arumugam, J., Senthil kumar, M., Prabu, H.J., Sundaram, S.J., Al-Dhabi, N.A., Arasu, M.V., Maaza, M., Kaviyarasu, K., 2020. Temperature effect on CuO nanoparticles: Antimicrobial activity towards bacterial strains. Surf. Interfaces 21, 100761. https://doi.org/10.1016/j.surfin.2020.100761.

George, A., Magimai Antoni Raj, D., Venci, X., Dhayal Raj, A., Albert Irudayaraj, A., Josephine, R.L., John Sundaram, S., Al-Mohaimeed, A.M., Al Farraj, D.A., Chen, T.-W., Kaviyarasu, K., 2022. Photocatalytic effect of CuO nanoparticles flower-like 3D nanostructures under visible light irradiation with the degradation of methylene blue (MB) dye for environmental application. Environ. Res. 203, 111880. https://doi.org/10.1016/j.envres.2021.111880.

Ghulam, M., Hajira, T., Muhammad, S., Nasir, A., 2013. Synthesis and characterization of cupric oxide (CuO) nanoparticles and their application for the removal of dyes. Afr. J. Biotechnol. 12 (47), 6650–6660.

Jayakumar, G., Irudayaraj, A.A., Raj, A.D., Sundaram, S.J., Kaviyarasu, K., 2022. Electrical and magnetic properties of Ni doped CeO_2 nanostructured for optoelectronic applications. J. Phys. Chem. Solids 160, 110369.

Jeyaram, R., Elango, A., Siva, T., Ayeshamariam, A., Kaviyarasu, K., 2020. Corrosion protection of silane-based coatings on mild steel in an aggressive chloride ion environment. Surf. Interfaces 18, 100423. https://doi.org/10.1016/j.surfin.2019.100423.

Jing, Z., Qinglin, X., Jinmin, L., 2012. Ferromagnetism in Fe doped CuO nanoparticle. J. Semicond. 33, 013001.

Joshua, J.P., Krishnan, S., Raj, D., Uthrakumar, R., Laxmi, S., Das, S.J., 2014. Novel synthesis of tenorite (CuO) nanoparticles by wet chemical method. Int. J. Chem. Tech. Res. 6, 22–33.

Kana, N., Kaviyarasu, K., Khamliche, T., Magdalane, C.M., Maaza, M., 2019. Stability and thermal conductivity of CuO nanowire for catalytic applications. J. Environ. Chem. Eng. 7 (4), 103255. https://doi.org/10.1016/j.jece:2019.103255.

Katti, V.R., Debnath, A.K., Muthe, K.P., Kaur, M., Dusa, A.K., Gadkari, S.C., 2003. Mechanism of drifts in H_2S sensing properties of SnO2: CuO composite thin film sensors prepared by thermal evaporation. Sens. Actuators B Chem. 245, 220–245.

Kaviyarasu, K., Devarajan, P.A., Xavier, S.S.J., Thomas, S.A., Selvakumar, S., 2012. One pot synthesis and characterization of cesium doped SnO_2 nanocrystals via a hydrothermal process. J. Mater. Sci. Technol. 28 (1), 15–20.

Kaviyarasu, K., Sajan, D., Devarajan, P.A., 2013. A rapid and versatile method for solvothermal synthesis of Sb2O3 nanocrystals under mild conditions. Appl. Nanosci. 3 (6), 529–533.

Kaviyarasu, K., Maria Magdalane, C., Anand, K., Manikandan, E., Maaza, M., 2015. Synthesis and characterization studies of MgO: CuO nanocrystals by wet-chemical method. Spectrochim. Acta Part A: Mol. Biomol. Spectroscopy 142, 405–409.

Kaviyarasu, K., Manikandan, E., Kennedy, J., Jayachandran, M., Ladchumananandasiivam, R., De Gomes, U.U., Maaza, M., 2016. Synthesis and characterization studies of NiO nanorods for enhancing solar cell efficiency using photon upconversion materials. Ceram. Int. 42 (7), 8385–8394.

Kayalvizhi, K., Alhaji, N.M.I., Saravanakkumar, D., Mohamed, S.B., Kaviyarasu, K., Ayeshamariam, A., Al-Mohaimeed, A.M., AbdelGawwad, M.R., Elshikh, M.S., 2022. Adsorption of copper and nickel by using sawdust chitosan nanocomposite beads–A kinetic and thermodynamic study. Environ. Res. 203, 111814. https://doi.org/10.1016/j.envres.2021.111814.

Khan, R.A., Beck, S., Dussault, D., Salmieri, S., Bouchard, J., Lacroix, M., 2013. Mechanical and barrier properties of nano crystalline cellulose reinforced poly (caprolactone) composites: effect of gamma radiation. J. Appl. Polym. Sci. 129, 3038–3046.

Kida, T., Oka, T., Nagano, M., Ishiwata, Y., Zheng, X.-G., 2007. Synthesis and application of stable copper oxide nanoparticle suspensions for nanoparticulate film fabrication. J. Am. Ceram. Soc. 90 (1), 107–110.

Kim, Y.-S., Hwang, I.-S., Kim, S.-J., Lee, C.-Y., Lee, J.-H., 2008. CuO nano wire gas sensors for air quality control in automotive cabin. J. Sens. Actuators, B 135 (1), 298–303.

Lee, S., Choi, U.S., Li, S., Eastman, J.A., 1999. Measuring thermal conductivity of fluids containing oxide nanoparticles. J. Heat Transfer 121, 280–289.

Lim, Y.-F., Choi, J.J., Hanrath, T., 2012. Facile synthesis of colloidal CuO nanocrystals for light harvesting applications. J. Nanomater. 2012, 1–6.

Liu, J., Huang, X., Li, Y., Sulieman, K.M., He, X., Sun, F., 2006. Hierarchical nanostructures of cupric oxide on a copper substrate: controllable morphology and wettability. J. Mater. Chem. 16 (45), 4427. https://doi.org/10.1039/b611691d.

Manimaran, R., Palaniradja, K., Alagumurthi, N., Sendhilnathan, S., Hussain, J., 2014. Preparation and characterization of copper oxide nanofluid for heat transfer applications. Appl. Nanosci. 4 (2), 163–167.

Mehedi Hassan, M., Khan, W., Azam, A., Naqvi, A.H., 2015. Influence of Cr incorporation on structural, Dielectric and optical properties of ZnO nanoparticles. J. Ind. Eng. Chem. 21, 283–291.

Nithiyavathi, R., John Sundaram, S., Theophil Anand, G., Raj Kumar, D., Dhayal Raj, A., Al Farraj, D.A., Aljowaie, R.M., AbdelGawwad, M.R., Samson, Y., Kaviyarasu, K., 2021. Gum mediated synthesis and characterization of CuO nanoparticles towards infectious disease-causing antimicrobial resistance microbial pathogens. J. Infect. Public Health 14 (12), 1893–1902.

S Panimalar, R Uthrakumar, E Tamil Selvi, P Gomathy, C Inmozhi, K Kaviyarasu, J Kennedy, Studies of MnO_2/g-C_3N_4 hetrostructure efficient of visible light photocatalyst for pollutants degradation by sol-gel technique, Surfaces and Interfaces 20, 100512, 2020.

Panimalar, S., Logambal, S., Thambidurai, R., Inmozhi, C., Uthrakumar, R., Muthukumaran, A., Rasheed, R.A., Gatasheh, M.K., Raja, A., Kennedy, J., Kaviyarasu, K., 2022. Effect of Ag doped MnO_2 nanostructures suitable for wastewater treatment and other environmental pollutant applications. Environ. Res. 205, 112560. https://doi.org/10.1016/j.envres.2021.112560.

Poizot, P., Laruelle, S., Grugeon, S., Dupont, L., Tarascon, J.-M., 2000. Nano-sized transition-metaloxides as negative-electrode materials for lithium-ion batteries. Nature 407 (6803), 496–499.

Poovendran, K., Wilson, K.S.J., Revathy, M.S., Ayeshamariam, A., Kaviyarasu, K., 2020. Functionalization effect of HAp with copper (Cu) having excellent dielectric applications. Surf. Interfaces 19, 100474. https://doi.org/10.1016/j.surfin.2020.100474.

Rahmana, M., Jamal, A., Bahadar Khan, S., Faisal, M., 2011. CuO doped ZnO based nanostructured materials for sensitive chemical sensor applications. ACS Appl. Mater. Interfaces 3, 1346–1351.

Ramesh, R., Yamini, V., Sundaram, S.J., Khan, F.L.A., Kaviyarasu, K., 2021. Investigation of structural and optical properties of NiO nanoparticles mediated by Plectranthus amboinicus leaf extract. Mater. Today:. Proc. 36, 268–272.

Rao, G.N., Yao, Y.D., Chen, J.W., 2007. Influence of Mn substitution on microstructure and magnetic properties of Cu1 – x Mn x O nanoparticles. J. Appl. Phys. 101 (9), 09H119. https://doi.org/10.1063/1.2714190.

Sowmya Sri Rathnakumar, Kana Noluthando, Arockia Jayalatha Kulandaiswamy, John Bosco Balaguru Rayappan, Kaviyarasu Kasinathan, John Kennedy, Malik Maaza, Stalling behaviour of chloride ions: a non-enzymatic electrochemical detection of α-Endosulfan using CuO interface, Sensors Actuators B: Chem. 293, (2019), 100-106.

Rehman, S., Mumtaz, A., Hasanain, S.K., 2011. size effects on the magnetic and optical properties of CuO nanoparticles. J. Nanopart. Res. 13 (6), 2497–2507.

Saravanakkumar, D., Sivaranjani, S., Kaviyarasu, K., Ayeshamariam, A., Ravikumar, B., Pandiarajan, S., Veeralakshmi, C., Jayachandran, M., Maaza, M., 2018. Synthesis and characterization of ZnO–CuO nanocomposites powder by modified perfume spray pyrolysis method and its antimicrobial investigation. J. Semicond. 39 (3), 033001. https://doi.org/10.1088/1674-4926/39/3/033001.

Saravanakkumar, D., Oualid, H.A., Brahmi, Y., Ayeshamariam, A., Karunanaithy, M., Saleem, A.M., Kaviyarasu, K., Sivaranjani, S., Jayachandran, M., 2019. Synthesis and characterization of CuO/ZnO/CNTs thin films on copper substrate and its photocatalytic applications. Open NANO 4, 100025. https://doi.org/10.1016/j.onano.2018.11.001.

Senthil, R., Vijayaragavan, G., Ayeshamariam, A., Kaviyarasu, K., 2020. Nonlinear optical properties of single crystal of L-OOMHCL incorporation with Glycine Oxalic Acid (GOA) with high chemical stability for optoelectronic applications. Surf. Interfaces 18, 100417. https://doi.org/10.1016/j.surfin.2019.100417.

Suleiman, M., Mousa, M., Hussein, A., Hammouti, B., Hadda, T.B., Warad, I., 2013. Copper (II)-oxide nanostructures: synthesis, characterizations and their applications review. J. Mater. Environ. Sci. 5, 792–807.

Theophil Anand, G., Renuka, D., Ramesh, R., Anandaraj, L., John Sundaram, S., Ramalingam, G., Magdalane, C.M., Bashir, A.K.H., Maaza, M., Kaviyarasu, K., 2019. Green synthesis of ZnO nanoparticle using Prunus dulcis (Almond Gum) for antimicrobial and supercapacitor applications. Surf. Interfaces 17, 100376. https://doi.org/10.1016/j.surfin.2019.100376.

Volanti, D.P., Keyson, D., Cavalcante, L.S., Simões, A.Z., Joya, M.R., Longo, E., Varela, J. A., Pizani, P.S., Souza, A.G., 2008. Synthesis and characterization of CuO flower-nanostructure processing by a domestic hydrothermal microwave. J. Alloy. Compd. 459 (1-2), 537–542.

Wang, H., Xu, J.-Z., Zhu, J.-J., Chen, H.-Y., 2002. Preparation of CuO nanoparticles by microwave irradiation. J. Cryst. Growth 244 (1), 88–94.

Yang, X., Chen, S., Zhao, S., Li, D., Ma, H., 2003. Synthesis of Copper Nanorods Using Electrochemical Methods. J. Serb. Chem. Soc. 68 (11), 843–847.

Yuan, G., Jiang, H., Lin, C., Liao, S., 2007. shape and controlled electrochemical synthesis of cupric oxide nano crystals. J. Cyst. Growth. 303, 400–406.

Zhang, W., Guo, F., Wang, F., Zhao, N., Liu, L., Li, J., Wang, Z., 2014. Synthesis of quinazolines via CuO nanoparticles catalyzed aerobic oxidative coupling of aromatic alcohols and amidines. J. Org. Biomol. Chem. 12 (30), 5752–5756.

Zheng, L., Liu, X., 2007. Solution-phase synthesis of CuO hierarchical nano sheets at near-neutral pH and near-room temperature. Mater. Lett. 61 (11-12), 2222–2226.

Zhou, Z., Lu, C., Wu, X., Zhang, X., 2013. Cellulose nanocrystals as a novel support for CuO nanoparticles catalysts: facile synthesis and their application to 4-nitrophenol reduction. RSC Adv. 3, 26066–26073.